Quantum efficiencies of bacteriorhodopsin photochemical reactions

Aihua Xie

Department of Physics, University of Illinois at Urbana-Champaign, Urbana, Illinois 61801 USA

ABSTRACT   Determination of quantum efficiencies of bacteriorhodopsin (bR) photoreactions is an essential step toward a full understanding of its light-driven proton-pumping mechanism. The bR molecules can be photoconverted into and from a K state, which is stable at 110 K. I measured the absorption spectra of pure bR, and the photoequilibrium states of bR and K generated with 420, 460, 500, 510, 520, 540, 560, 570, 580, 590, and 600 nm illumination at 110 K. The fraction of the K population in the photoequilibrium state, f_K, is determined by A_{bR} and A_K, the absorbances of the bR and K states at the excitation wavelengths, and also by ϕ_1 and ϕ_2, the quantum efficiencies for the bR to K and K to bR photoconversions: $f_K = \phi_1 A_{bR}/(\phi_1 A_{bR} + \phi_2 A_K)$. By assuming that the ratio ϕ_1/ϕ_2 is the same at two different but close wavelengths, for example 570 and 580 nm, the value of ϕ_1/ϕ_2 at 570 and 580 nm was determined to be 0.55 ± 0.02, and the spectrum of the K state was obtained with the peak absorbance at 607 nm. The values of ϕ_1/ϕ_2 at the other excitation wavelengths were then evaluated using the known K spectrum, and show almost no dependence on the excitation wavelength within the main band. The result $\phi_1/\phi_2 = 0.55 ± 0.02$ disagrees with those of many other groups. The advantages of this method over others are its minimal assumptions and its straightforward procedure.

INTRODUCTION

Bacteriorhodopsin (bR) is a light-energy transducer (1, 2). When bR is in its light-adapted state, it absorbs photons and uses the energy of the captured photons to pump protons outwards across the cell membrane. The energy stored in the resulting proton gradient may then be used for bioenergetic processes in the cell. Determination of quantum efficiencies of bR photoreactions is an essential step toward a full understanding of the pumping mechanism: the quantum efficiencies bear on such basic questions as how many protons are pumped in one photocycle and what are the spectral and dynamic characteristics of photocycle intermediates formed during the proton pumping process. Oesterhelt and Hess reported the first measurement of a quantum yield, determining that of the M intermediate to be 0.79 using an ether-saturated solvent in high salt concentration to slow down the decay of M (3). Since then, the quantum efficiencies of the bR photoreactions have been studied by many other groups (4–14; Xie, A., R. A. Bogomolni, and W. Stoeckenius, manuscript in preparation). However, the results are controversial: the reported values of the quantum efficiency of bR to K or bR to M photoconversion vary from 0.25 ± 0.05 (7) to 0.79 (3), and the ratio of quantum efficiencies of the forward and backward photoreactions between bR and K varies from 0.34 (11) to 0.79 (3). Birge et al. (9) tabulated many of the reported results providing an overall view. The difficulties in determination of quantum efficiencies of bR photoreactions are due to

several reasons: the photoreactions are reversible, and the spectra of the photocycle intermediates of bR, except for the M intermediate, are strongly overlapping with that of bR, while the M intermediate cannot be separated in time from the O and N intermediates. Consequently, one needs to make some assumptions either explicitly or implicitly to determine the quantum efficiencies of bR photoreactions. The inadequacies in assumptions made in data analysis are among the major causes for the diversity in the experimental results.

At physiological temperatures, the photoreaction of bR leads to a sequence of thermal transitions involving major intermediates, namely I, J, K, L, M, N, and O (15–17), and finally the molecule returns to the bR state. This photon triggered sequence is the photocycle. The photocycle of bR has not been fully understood yet, even after extensive studies. However, at low temperatures, for example, 110 K, the lifetime of the K intermediate is as long as 30 yr predicted from the K to L transition observed from 140 to 160 K and there is no K to L transition observed within hours below 125 K (unpublished results). The K state is stable at 110 K, while its risetime is ~36 ps even at 4 K (18). Therefore, I avoid the complication of the bR photocycle by performing the experiment at 110 K, at the temperature where only the K state is populated and stabilized upon the photoreaction of bR. On the other hand, I developed the method of E. Fischer (19) to determine the ratio of quantum effi-

ciencies of the photoreactions between bR and K using only one reasonable assumption. This assumption will be shown valid for the bR case in Results and Discussion.

PRINCIPLES AND METHODS

The photoreaction of bR at 110 K can be characterized by Scheme 1. The photoproduct of bR is the K state which is stable at 110 K and can be photoconverted back to bR. The quantum efficiency ϕ_1 is the probability for bR to K photoconversion after absorbing a photon, whereas the quantum efficiency ϕ_2 is the one for K to bR photoconversion. Photoequilibrium between the bR and K states can

$$bR \underset{\phi_2}{\overset{\phi_1}{\rightleftharpoons}} K$$
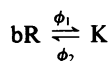
Scheme 1

be achieved by an extensive illumination so that further photo-excitation will no longer change the populations of the bR and K states. For excitation wavelength λ_e the fraction of the K population in photoequilibrium $f_K(\lambda_e)$ is determined by

$$
\begin{aligned}
f_K(\lambda_e) &= \frac{\phi_1 \epsilon_{bR}(\lambda_e)}{\phi_1 \epsilon_{bR}(\lambda_e) + \phi_2 \epsilon_K(\lambda_e)} \\
&= \frac{\phi_1 A_{bR}(\lambda_e)}{\phi_1 A_{bR}(\lambda_e) + \phi_2 A_K(\lambda_e)},
\end{aligned}
\tag{1}
$$

where $\epsilon_{bR}(\lambda_e)$ and $\epsilon_K(\lambda_e)$ are the extinctions of the bR and K states, while $A_{bR}(\lambda_e)$ and $A_K(\lambda_e)$ are the absorbances. The K to bR difference spectrum obtained from the photoequilibrium state generated by extensive illumination at λ_e, $\Delta A_K(\lambda, \lambda_e)$, is proportional to the fraction of the K population:

$$
\begin{aligned}
\Delta A_K(\lambda, \lambda_e) &\equiv A_{K+bR}(\lambda, \lambda_e) - A_{bR}(\lambda) \\
&= f_K(\lambda_e)[A_K(\lambda) - A_{bR}(\lambda)],
\end{aligned}
\tag{2}
$$

where λ is the measuring wavelength and $A_{K+bR}(\lambda, \lambda_e)$ is the absorption spectrum of the photoequilibrium state. By assuming only that the ratio of quantum efficiencies ϕ_1/ϕ_2 is the same at two different excitation wavelengths, λ_e^1 and λ_e^2, one can determine the ratio ϕ_1/ϕ_2, the fraction of the K population, $f_K(\lambda_e)$, and the absorption spectrum of the K state, $A_K(\lambda)$, using the following procedure.

The amplitude of the K to bR difference absorbance spectrum $\Delta A_K(\lambda, \lambda_e)$ is proportional to the fraction of the K population, $f_K(\lambda_e)$. The ratio $f_K(\lambda_e^1)/f_K(\lambda_e^2)$ is equal to the ratio of the peak-to-peak amplitudes of the K to bR difference spectra for the photoequilibrium states after excitations at wavelengths λ_e^1 and λ_e^2, and therefore can be determined directly from spectral measurement. Using a trial and error procedure, one assigns a trial value $f_K^{(i)}(\lambda_e^1)$ to $f_K(\lambda_e^1)$, calculates the corresponding absor-

bances of the K state at λ_e^1 and λ_e^2, $A_K^{(i)}(\lambda_e^1)$ and $A_K^{(i)}(\lambda_e^2)$ using Eq. 2. The ratio $(\phi_1/\phi_2)^{(i)}$ can be calculated from the trial $f_K^{(i)}(\lambda_e^1)$ and the resulting $A_K^{(i)}(\lambda_e^1)$. The corresponding $f_K^{(i)}(\lambda_e^2)$ is obtained from the calculated ratios $(\phi_1/\phi_2)^{(i)}$ and $A_K^{(i)}(\lambda_e^2)/A_{bR}(\lambda_e^2)$ using Eq. 1. When the resulting ratio $f_K^{(i)}(\lambda_e^1)/f_K^{(i)}(\lambda_e^2)$ equals the observed ratio $f_K(\lambda_e^1)/f_K(\lambda_e^2)$, the values of $f_K^{(i)}(\lambda_e^1)$ and $f_K^{(i)}(\lambda_e^2)$ are the actual values of $f_K(\lambda_e^1)$ and $f_K(\lambda_e^2)$. At the same time, the K spectrum and the ratio of quantum efficiencies are also determined. Note that only about four trials are needed to obtain the final results because one can estimate about how close and in which direction the last trial value $f_K^{(i)}(\lambda_e^1)$ is to the actual value $f_K(\lambda_e^1)$ from the first two trials.

The method described here is not limited to the bR $\rightleftharpoons$ K photoequilibrium system, but is general to any A $\rightleftharpoons$ B photoequilibrium system when only A is known. E. Fischer found an exact analytical solution for the fraction of the B (or K) population (19). Of course, there also exists the exact analytical solution for the ratio of quantum efficiencies ϕ_1/ϕ_2. The numerical method developed here is more intuitive and straightforward compared with the formulation of the exact analytical solutions. With this method, the ratio ϕ_1/ϕ_2, the fraction of the K population, and the K spectrum are determined at the same time. The criteria for optimal results using this method are as follows.

The first criterion concerns the validity of the assumption that the quantum efficiencies are the same at the two chosen excitation wavelengths. The quantum efficiencies might depend on the excitation wavelength only if more than one electronic transition is involved (20). In the case that there is more than one transition and these transitions have different quantum efficiencies, the errors due to the assumption can be minimized by choosing two excitation wavelengths close enough. The second criterion concerns the sensitivity of the ratio ϕ_1/ϕ_2 to the excitation wavelength. If the ratio ϕ_1/ϕ_2 is the same at the two chosen excitation wavelengths, the ratio ϕ_1/ϕ_2 has the form

$$
\frac{\phi_1}{\phi_2} = \frac{(A_K/A_{bR})_{\lambda_e^1} f_K(\lambda_e^1)/f_K(\lambda_e^2) - (A_K/A_{bR})_{\lambda_e^2}}{1 - f_K(\lambda_e^1)/f_K(\lambda_e^2)}
\tag{3}
$$

derived from Eq. 1. If the ratio A_K/A_{bR} is identical at the two excitation wavelengths, the fraction of the K population is also the same at these two wavelengths. In this case, the ratio ϕ_1/ϕ_2 is indeterminate because both the denominator and numerator in the above equation becomes zeroes. The more the ratio A_K/A_{bR} differs at the two chosen excitation wavelengths, the better the sensitivity in determination of the ratio ϕ_1/ϕ_2. Therefore, the calculation of the ratio ϕ_1/ϕ_2 should be optimized by choosing two such excitation wavelengths that are very

close to each other so that any possible errors due to the wavelength dependence of the ratio ϕ_1/ϕ_2 will be small, and on the other hand yield a large difference in the ratio A_K/A_{bR} to ensure good sensitivity in determination of the ratio ϕ_1/ϕ_2.

MATERIALS AND METHODS

Purple membrane purified from strain S9 of *Halobacterium halobium* (21) was kindly provided by Professor T. Ebrey and Dr. R. Govindjee. The purple membrane suspension was prepared in 70% glycerol/water (vol/vol) buffered to pH 7 with 10 mM potassium phosphate. The glycerol was used to prevent sample cracking at low temperatures. The bR sample had a 1.66 OD peak absorbance at 577 nm at 110 K in a 1-cm pathlength cell.

The bR sample in a $1 \times 1 \times 4$ cm^3 plastic cuvette was loaded into the sample chamber of an 8 DT storage optical dewar (Janis Research Company Inc., Wilmington, MA) equipped with four quartz windows. The sample temperature was controlled by a DRC 93C temperature controller (Lake Shore Cryotronics Inc., Westerville, OH). The optical tail of the dewar was placed in the sample chamber of an Olis-Cary 14 spectrophotometer, interfaced to an IBM PC/AT (On-Line Instrument Systems, Inc., Jefferson, GA). Each spectrum was scanned from 770 to 370 nm in 2-nm intervals. The absorbances of both the bR and K states are negligible at 770 nm. The wavelength accuracy and wavelength reproducibility are 0.4 and 0.05 nm, respectively for the Cary-14 spectrophotometer. The wavelength resolution of the monitoring beam is better than 0.08 nm determined from the slit width (0.02 mm) in the spectral region from 470 to 670 nm, and is reduced slightly to 0.11 at 770 nm and to 0.14 nm at 370 nm. A 250-W tungsten lamp (model 66181; Oriel Corp., Stratford, CT) was used to light-adapt the bR sample and to generate photoequilibrium states of K and bR. The actinic beam from this lamp was perpendicular to the monitoring beam of the spectrophotometer. The optical pathlengths for the excitation beam and the monitoring beam are the same, both 1 cm. The optical alignment was made such that the monitoring beam path of the Cary-14 inside the sample is close to the actinic lamp for fast photoequilibrium. A 7.5-cm water filter reduced sample heating by the illumination light. Interference filters were used in the actinic beam to obtain monochromatic light at the desired wavelengths. The transmission spectra of the filters were also measured in the Olis-Cary 14 spectrophotometer.

The bR sample was light-adapted with white light at room temperature for 200 s, then cooled to 260 K and light-adapted again for 600 s. At 260 K the dark-adaptation process is very slow and the bR photocycle is completed in ~15 min. The bR sample remained at 260 K for 28 min after the illumination, while the completion of the photocycle was checked. The bR sample was then further cooled to 110 K in the dark. After the sample was thermally stabilized at 110 K for 10 min, a spectrum of bR was taken. Then the sample was illuminated in sequence at selected wavelengths using narrow band interference filters (6–10 nm in bandwidths) to generate the photoequilibrium states of bR and K, and the spectrum of each photoequilibrium state was collected. The duration of illumination required for photosaturation is determined by both the light intensity of the actinic beam inside the sample and the extinctions of the bR and K states at the excitation wavelength. Typically 99.9% photosaturation was achieved in 30 s at 570 nm and in 250 s at 420 nm. The photoequilibration was also carried out at 460, 500, 510, 520, 540, 560, 580, 590, and 600 nm. At the end, a background spectrum of the solvent only (70% glycerol/water [vol/vol] with 10 mM potassium phosphate) was measured at 110 K using the same plastic cuvette as for the bR sample.

Because of the finite bandwidth of the illumination light, the excitation wavelength used for the data evaluation is the mean transmission

wavelength of the interference filter corrected by the radiation spectrum of the halogen tungsten lamp approximated by the black body radiation at 3,270 K. The emission from the lamp is more intense in the red than in the blue. Therefore, the illumination wavelengths are ~0.05 nm longer than the mean transmission wavelength of the filters. The eleven excitation wavelengths are found at 420.53, 460.30, 500.23, 511.03, 520.28, 539.62, 561.86, 570.32, 580.09, 590.64, and 600.48 nm.

RESULTS AND DISCUSSION

The spectrum of the pure bR state at 110 K was baseline corrected by subtracting the background spectrum of the solvent. The peak absorbance of bR is found at 577 nm as shown in Fig. 1. Fig. 2 shows the K to bR difference spectra between the photoequilibrium state and the bR state obtained from illumination at 500, 570, and 600 nm. These difference spectra are similar in shape with a maximum at 632 nm and a minimum around 554 nm, indicating that only two states, K and bR, are involved in the photoequilibrium. The relative K populations in the photoequilibrium states were calculated for all excitation wavelengths by comparing the amplitudes of the K to bR difference spectra, and the results are shown in Fig. 3. Excitation at 510 nm gives the highest K state population.

Data evaluation is optimized by choosing a pair of proper excitation wavelengths. The fraction of the K population changes little from 500 to 520 nm (Fig. 3), therefore, the data evaluation method has a poor sensitivity in this region. The change of the fraction of the K population from 560 to 570 nm is also small compared with that of neighboring wavelengths. Although such changes are large from 580 to 600 nm, however, the absorbance of bR decreases sharply as the wavelength increases from 580 to 600 nm. The finite bandwidth and/or a small error in determination of the illumination wavelength may therefore yield a large error in the ratio of the quantum efficiencies. Consequently the excitation wavelengths 570 and 580 nm are first chosen for the data
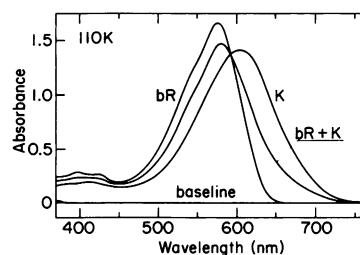

FIGURE 1 The absorption spectra of the light-adapted bR and the photoequilibrium state of K and bR from excitation at 570 nm, both are baseline corrected by subtracting the background spectrum of the solvent (70% glycerol/water [vol/vol] with 10 mM potassium phosphate). The evaluated K spectrum from photoequilibration at 570 and 580 nm is also included. All the spectra shown are collected at 110 K.
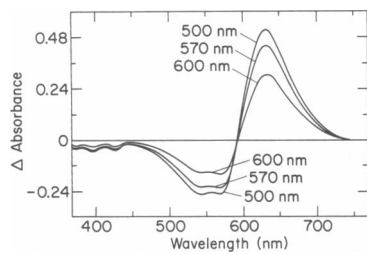
FIGURE 2 The K to bR difference spectra obtained from photoequilibration at 500, 570, and 600 nm. The K to bR isosbestic points are at 592.04, 592.93, and 593.92 nm, respectively.

evaluation. These two wavelengths are only 10 nm apart; the errors due to any wavelength dependence of the ratio will be small. The isosbestic point between bR and K shifts by 0.3 nm from photoequilibrium at 570 to 580 nm. Such difference in the isosbestic point can be interpreted as spectral hole-burning (22, 23). Following the procedure already described, the values of ϕ_1/ϕ_2 calculated from the K to bR difference spectra for photoequilibration at 570 and 580 nm are 0.58 and 0.52, respectively. Such errors in the ratio due to the spectral hole-burning are reduced by using an averaged difference spectrum: scale the amplitude of the one difference spectrum to another and then take the average. The final value of ϕ_1/ϕ_2 is found to be 0.55 ± 0.02 at 570 and 580 nm, whereas the fraction of the K population is 44.4 ± 0.9% at 570 nm and 42.1 ± 1.0% at 580 nm. The resulting K spectrum is shown in Fig. 1. It has a peak absorbance of 607 nm with a relative peak height of 0.84 as compared with bR. Detailed error analysis is presented in the Appendix.

The fraction of the K population at other excitation wavelengths are calculated by comparing the ratio of the peak-to-peak amplitudes of the K to bR difference spectra. The ratio of the quantum efficiencies ϕ_1/ϕ_2 is then
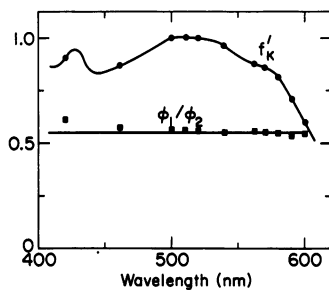
determined from the known fraction of the K population and the K to bR difference spectra. The resulting ratio ϕ_1/ϕ_2 and the fraction of the K population are listed in Table 1. To check the self consistency of the results, a pair of the excitation wavelengths 540 and 560 nm were chosen to calculate the ratio ϕ_1/ϕ_2. The resulting value of the ratio ϕ_1/ϕ_2 is 0.54 ± 0.02 at 540 and 560 nm, in agreement with that shown in Table 1 within errors. The maximum fraction of the K population is 52% for illumination at 500–520 nm. Therefore, these wavelengths are good for photoexcitations in flash photolysis experiment to achieve the largest signals. The relative absorbance of K to bR, an important parameter in the calculation of the quantum efficiencies, is also included in Table 1.

The validity of the assumption that the ratio ϕ_1/ϕ_2 is the same at 570 and 580 nm can now be examined. A very low temperature bR spectrum (~10 K) shows at least three transition lines within the main band (577 nm). The relative contributions of the three transition lines to the photoequilibrium are strongly dependent on the excitation wavelength. If the ratio ϕ_1/ϕ_2 is different for the three transition lines across the main band, the resulting ratio ϕ_1/ϕ_2 would depend on the excitation wavelength except at 570 and 580 nm, where the ratio ϕ_1/ϕ_2 is forced to be identical. The fact that the ratio ϕ_1/ϕ_2 is fairly constant from 500 to 600 nm as shown in Fig. 3 and Table 1 proves the excellent validity of the assumption.

The ratio ϕ_1/ϕ_2 is 0.61 at 420 nm, slightly higher than the value for the main band, 0.55. It is unclear whether this difference in the ratio is real or due to membrane scattering. Balashov et al. reported a bR spectrum with a blue to red peak ratio of 0.14 (12), smaller than 0.17, the ratio from the bR spectrum shown in Fig. 1. However, I found that the spectral distortion due to membrane scattering is negligible by comparison of the two bR spectra taken with the sample cuvette placed in the two extreme positions along the monitoring beam, close to and

FIGURE 3 The relative population of the K state f'_K (●) and the ratio of quantum efficiencies ϕ_1/ϕ_2 (■) via excitation wavelengths. The solid line for the relative population of the K state was calculated using Eq. 1 from the values of $A_K(\lambda)/A_{bR}(\lambda)$ and ϕ_1/ϕ_2 of the neighboring excitation wavelengths.

TABLE 1 The ratio of quantum efficiencies, ϕ_1/ϕ_2, the fraction of the K population, $f_K(\lambda_e)$, and the ratio of the K to bR absorbances, $A_K(\lambda_e)/A_{bR}(\lambda_e)$, at 110 K

λ_e	ϕ_1/ϕ_2	f_K (%)	A_K/A_{bR}
nm			
420.45	0.609 ± 0.022	46.8 ± 0.8	0.693
461.24	0.572 ± 0.022	44.9 ± 0.8	0.702
500.18	0.562 ± 0.030	51.7 ± 1.0	0.526
510.98	0.553 ± 0.023	51.8 ± 1.0	0.516
520.23	0.561 ± 0.023	51.6 ± 0.8	0.525
539.57	0.555 ± 0.021	49.2 ± 0.8	0.573
561.81	0.553 ± 0.020	45.3 ± 0.8	0.668
570.28	0.549 ± 0.020	44.4 ± 0.9	0.688
580.04	0.545 ± 0.024	42.1 ± 1.0	0.751
590.59	0.535 ± 0.030	36.7 ± 1.3	0.924
600.42	0.544 ± 0.036	30.9 ± 1.3	1.215

far from the photomultiplier in the sample chamber of the Cary-14 spectrophotometer. If this difference in the ratio is real, it indicates that the electronic transitions for the blue band do not relax to the same lowest electronic excited state as the transitions of the main band, before any relaxations toward the first electronic ground state. Such a transition could have a different ratio ϕ_1/ϕ_2 than that of the main band.

The results that the ratio $\phi_1/\phi_2 = 0.55 \pm 0.02$ and the maximum fraction of the K population is $51.8 \pm 1.0\%$ obtained here are in agreement with those $\phi_1/\phi_2 = 0.5 \pm 0.1$ and the maximum $f_K = 53 \pm 4\%$ found by Balashov and Litvin (12), but the uncertainties in their data are larger. The evaluated ratio ϕ_1/ϕ_2 sets an upper limit for the quantum efficiency ϕ_1 as 0.64 for the blue band and 0.57 for the main band. The value of the quantum efficiency ϕ_1 calculated by Schneider et al. is 0.67 from resonance Raman scattering measurement with excitations at 502, 514, 568, and 647 nm (12). This value ($\phi_1 = 0.67$) is larger than the upper limit of the ϕ_1 (≤ 0.57) because they neglected the photoselection effect (see reference 24) in their data evaluation. An early measurement by Hess and Oesterhelt (3) gave a value of 0.79 for the quantum yield of the M state, whereas a recent report by Tittor and Oesterhelt (14) provided a lower limit of the quantum yield of the M state as 0.64 ± 0.04. No explicit reasons can be found to explain such discrepancy between their value and the upper limit given here. However, the method applied here is rather straightforward, and the errors in the ratio ϕ_1/ϕ_2 and in the upper limit of the quantum efficiency ϕ_1 are very small, only ± 0.02.

The other values of the quantum efficiency ϕ_1 as previously reported range from 0.25 to 0.49, and do not exceed the upper limit 0.57 given here. However, their fraction of the K population or their fraction of photocycling are smaller than my results. Note that many of them employed the M intermediate for their data evaluation (3, 4, 6–8). Because there is an L to bR branch reaction at low temperatures (25, 26), the quantum yield of M is smaller than the quantum yield of K. At room temperature, the bR photocycle is not well understood, and the M intermediate cannot be separated in time from the O and/or N intermediate under normal conditions. The errors introduced by using inappropriate models for the bR photocycle are unknown. Another error source in evaluation of the quantum efficiency is neglecting the photoselection effect. Due to the nature of light as an electromagnetic transverse wave, photoselection always exists and should be considered because there are no photons with polarization parallel to the beam direction. In using a photosaturation method at room temperature (4, 10, 11), one should determine the degree of saturation in terms of the dichroic ratio (Xie, A., R. A. Bogomolni,

and W. Stoeckenius, manuscript in preparation), not by the fraction of the K population. Because of photoselection, photosaturation of the bR molecules with transition dipoles perpendicular to the electric vector(s) of the excitation beam requires a much higher intensity than that for bR molecules with transition dipoles parallel to the electric vector(s) of the excitation light. The bR sample might even be partially bleached before reaching full photosaturation (unpublished results with P. Ormos).

Finally, it should be pointed out that the absolute quantum efficiencies ϕ_1 and ϕ_2 can be measured at any excitation wavelength with the known extinction coefficient of bR (27) because the ratio ϕ_1/ϕ_2 and the absorption spectrum of the K state have been determined here. We have already finished a measurement of the absolute quantum efficiencies $\phi_1 + \phi_2$ using a photoselection method (Xie, A., R. A. Bolgomolni, and W. Stoeckenius, manuscript in preparation). The values of the quantum efficiencies ϕ_1 and ϕ_2 can therefore be evaluated from the ratio ϕ_1/ϕ_2 and the sum $\phi_1 + \phi_2$. The method for quantum efficiency measurement described in the paper has advantages over others for its minimal assumptions and its straightforward procedure, and it can be applied to any $A \rightleftharpoons B$ photoreaction system when only A is known, such as halorhodopsin and sensor rhodopsin.

APPENDIX

Error analysis

The bR spectrum shown in Fig. 1 was baseline corrected by subtracting a background spectrum of the solvent. The background spectrum shown in Fig. 1 is fairly constant in the visible region and shows increasing absorbance in the near-UV due to cuvette absorbance. The random noise in the bR spectrum is ≤ 0.6 milli OD in the region from 550 to 600 nm, only $\leq 0.04\%$ of the bR absorbance there, and is 0.2 milli OD in the other region. The random noise in the peak-to-peak amplitude of the K to bR difference spectrum is 0.5 milli OD, $\sim 0.07\%$ of the signal for photoequilibrium at 570 and 580 nm. The resulting error in the ratio ϕ_1/ϕ_2 is ~ 0.002, and that in the fraction of the K population is $\sim 0.08\%$.

The systematic errors are mainly due to the finite bandwidth of illumination light and the spectral hole-burning effect, and are larger than the random errors. The band widths of the interference filters vary from 6 nm (in the blue) to 10 nm (in the red). The finite bandwidth would introduce errors only if the ratio A_K/A_{bR} varies with wavelength within the transmission band and such a variation in the ratio A_K/A_{bR} is asymmetric about the mean wavelength of the transmission band of the filter. The error in the ratio A_K/A_{bR} due to finite bandwidth is 0.93% at 570 nm and 1.6% at 580 nm. The resulting error in the ratio ϕ_1/ϕ_2 is 0.005 at 570 nm and is 0.009 at 580 nm. The isosbestic point between K and bR shifts slightly as the excitation wavelengths: 592.04 nm if excited at 500 nm and 593.92 nm if excited at 600 nm, as shown in Fig. 2. This phenomenon is due to spectral hole-burning and implies that the spectra are inhomogeneously broadened (22, 23). The errors due to the spectral hole-burning is reduced by using the averaged K to bR difference spectrum at 570 and 580 nm as described earlier. The errors in the fraction of the K population due to incomplete photosaturation and the K contamination in the bR spectrum was estimated to be 0.1%. The spectral distortion from membrane scattering was found to be negligible

by comparing the two bR spectra taken with the sample cuvette placed in the two extreme positions along the monitoring beam, close to and far from the photomultiplier in the sample chamber of the Cary-14 spectrophotometer. The nonlinearity of the system response is < -0.001 OD for absorbance ≤ 1.0 OD, and is ~ -0.006 OD for the peak absorbance of bR (1.66 OD) (28). Therefore, it contributes only small errors to the quantum efficiency evaluation. Because the same spectrophotometer was used for the transmission spectra of filters and the absorption spectra of bR and the photoequilibrium states of bR and K, the wavelength accuracy of the Cary-14 spectrophotometer does not introduce extra errors to the ratio ϕ_1/ϕ_2, but only causes a shift in the spectral wavelength. All of the sources of errors mentioned above were taken into account in the uncertainty analysis.

REFERENCES

1. Stoeckenius, W., R. H. Lozier, and R. A. Bogomolni. 1979. Bacteriorhodopsin and the purple membrane of *halobacteria. Biochim. Biophys. Acta.* 505:215–278.

2. Stoeckenius, W., and R. A. Bogomolni. 1982. Bacteriorhodopsin and related pigments of *halobacteria. Annu. Rev. Biochem.* 52:587–616.

3. Oesterhelt, D., and B. Hess. 1973. Reversible photolysis of the purple complex in the purple membrane of *Halobacterium halobium. Eur. J. Biochem.* 37:316–326.

4. Goldschmidt, C. R., M. Ottolenghi, and R. Korenstein. 1976. On the primary quantum yields in the bacteriorhodopsin photocycle. *Biophys. J.* 16:839–843.

5. Lozier, R. H., and W. Niederberger. 1977. The photochemical cycle of bacteriorhodopsin. *Fed. Proc.* 36:1805–1809.

6. Becher, B., and T. G. Ebrey. 1977. The quantum efficiency for the photochemical conversion of the purple membrane protein. *Biophys. J.* 17:185–191.

7. Goldschmidt, C. R., O. Kalisky, T. Rosenfeld, and M. Ottolenghi. 1977. The quantum efficiency of the bacteriorhodopsin photocycle. *Biophys. J.* 17:179–183.

8. Hurley, J. B., and T. G. Ebrey. 1978. Energy transfer in the purple membrane of *Halobacterium halobium. Biophys. J.* 22:49–66.

9. Birge, R. R., T. M. Cooper, A. F. Lawrence, M. B. Masthy, C. Vasilakis, C.-F. Zhang, and R. Zidovetski. 1989. A spectroscopic, photocalorimetric, and theoretical investigation of the quantum efficiency of the primary event in bacteriorhodopsin. *J. Am. Chem. Soc.* 111:4063–4074.

10. Dioumaev, A. K., V. V. Savransky, N. V. Tkachenko, and V. I. Chukharev. 1989. Quantum yield and extinction measurements in strongly overlapping reactant and photoproduct absorption bands. I: analytical method. *J. Photochem. Photobiol. B Biol.* 3:385–395.

11. Dioumaev, A. K., V. V. Savransky, N. V. Tkachenko, and V. I. Chukharev. 1989. Quantum yield and extinction measurements in strongly overlapping reactant and photoproduct absorption bands. II: bathointermediate formation in bacteriorhodopsin photocycle at room temperature. *J. Photochem. Photobiol. B Biol.* 3:397–410.

12. Balashov, S. P., and F. F. Litvin. 1981. Photochemical conversions of bacteriorhodopsin. *Biophysics (Poland).* 26:566–581.

13. Schneider, A., R. Diller, and M. Stockburger. 1989. Photochemical quantum yield of bacteriorhodopsin from resonance raman scattering as a probe for photolysis. *Chem. Phys. North-Holland, Amsterdam.* 131:17–29.

14. Tittor, J., and D. Oesterhelt. 1990. The quantum yield of bacteriorhodopsin. *FEBS (Fed. Eur. Biochem. Soc.) Lett.* 263:269–273.

15. Lozier, R. H., R. A. Bogomolni, and W. Stoeckenius. 1975. Bacteriorhodopsin: a light-driven proton pump in *Halobacterium halobium. Biophys. J.* 15:955–962.

16. Kouyama, T., A. Nasuda-Kouyama, A. Ikegami, M. K. Mathew, and W. Stoeckenius. 1988. Bacteriorhodopsin photoreaction: identification of a long-lived intermediate N (P, R$_{350}$) at high pH and its M-like photoproduct. *Biochemistry.* 27:5855–5863.

17. Sharkov, A. V., A. V. Pakulev, S. V. Chekalin, and Y. A. Matveetz. 1985. Primary events in bacteriorhodopsin probed by subpicosecond spectroscopy. *Biochim. Biophys. Acta.* 808:94–102.

18. Applebury, M. L., K. S. Peters, and P. M. Rentzepis. 1978. Primary intermediates in the photochemical cycle of bacteriorhodopsin. *Biophys. J.* 23:375–382.

19. Fischer, E. 1967. The calculation of photostationary states in systems A $\rightleftharpoons$ B when only A is known. *J. Phys. Chem.* 71:3704–3706.

20. Turro, N. J. 1965. Molecular Photochemistry. Benjamin, New York. 5.

21. Becher, B. M., and J. Y. Cassium. 1975. Improved isolation procedures for the purple membrane of *Halobacterium halobium. Prep. Biochem.* 5:161–178.

22. Cooper, A. 1983. Photoselection of conformational substates and the hypsochromic photoproduct of rhodopsin. *Chem. Phys. Lett.* 99:305–309.

23. Ormos, P., D. Braunstein, M. K. Hong, S.-L. Lin, and J. Vittitow. 1986. Hole burning in bacteriorhodopsin. *In* Biophysical Studies of Retinal Proteins. T. Ebrey, H. Frauenfelder, B. Honig, and K. Nakanishi, editors. University of Illinois Press, Urbana, IL. 238–247.

24. Nagle, J. F., S. M. Bhattacharjee, L. A. Parodi, and R. H. Lozier. 1983. Effect of photoselection upon saturation and the dichroic ratio in flash experiment upon effectively immobilized systems. *Photochem. Photobiol.* 38:331–339.

25. Iwasa, T., F. Tokunaga, and T. Yoshizawa. 1980. A new pathway in the photoreaction cycle of trans-bacteriorhodopsin and the absorption spectra of its intermediates. *Biophys. Struct. Mech.* 6:253–270.

26. Kalisky, O., M. Ottolenghi, B. Honig, and K. Korenstein. 1981. Environmental effects on formation and photoreaction of the M$_{412}$ photoproduct of bacteriorhodopsin: implications for the mechanism of proton pumping. *Biochemistry.* 20:649–655.

27. Rehorek, M., and M. P. Heyn. 1979. Binding of *all-trans*-retinal to the purple membrane. Evidence for cooperativity and the determination of the extinction coefficient. *Biochemistry.* 18:4977–4983.

28. Ansari, A. 1988. Conformational relaxation and kinetic hole-burning in sperm whale myoglobin. Ph.D. thesis. University of Illinois at Urbana-Champaign. 33.